1st Virtual European Conference on Fracture

Electromechanical contact elements for modelling adhesion and interfacial interactions in electrospun nanofibers systems

Claudio Maruccio[a,b,*], Adnan Kefal[c]

[a]*Faculty of Naval Architecture and Ocean Engineering, Istanbul Technical University, Istanbul, Turkey*
[b]*Department of Innovation Engineering, University of Salento, Lecce, Italy*
[c]*Faculty of Engineering and Natural Sciences, Sabanci University, Tuzla, Istanbul, Turkey*

Abstract

The analysis of deformation and interactions during the electromechanical contact between surfaces with non-matching meshes is important for advanced applications such as mechanical energy harvesting and pressure/force sensors using flexible piezoelectric devices made of polymeric nanowires. The node-to-segment (NTs) and the node-to-surface (NTS) algorithms are widely employed discretization techniques despite well known limitations in problems where the identification of the master segment/surface related to a slave-node is ambiguous or impossible. The objectives of this work is to extend the classical formulation to electromechanical interfaces using automatic differentiation technologies to derive and implement the resulting numerical equations. In particular, the contact contributions to the stiffness matrix and to the residual vector are derived and an adhesion behaviour is also added into the constitutive law. Then, some applications to selected practical problems are presented.

1. Introduction

Piezoelectric devices are attractive for several technological solutions, most notably for micro-electro-mechanical (MEMS) and nano-electro-mechanical (NEMS) systems with applications in human motion monitoring, robotics, sensing and energy harvesting, see [4, 18]. Recently, several numerical [1, 3, 9], experimental [2], and analytical [6, 10, 11] studies, focused on converting mechanical energy (i.e. vibrations) into electrical energy, are developed. In particular, energy harvesting techniques based on piezoelectric materials have been proven to be a viable method for charging small electronic devices for structural health monitoring applications, at different scales. From a device perspective, smart systems can exploit both the d_{31} [12, 22] or d_{33} [21] working mode. Furthermore, numerous electromechanical demonstrators have been built in the last ten years, with scale lengths ranging from nano to micro, up

* Corresponding author
    E-mail address: claudio.maruccio@unisalento.it

to macro levels. For example, Fan et al. [18] demonstrated that the piezoelectric effect works efficiently at the scale of single or arrays of nanowires; an high sensitivity accelerometer, composed of ultralong vertically aligned barium titanate nanowire arrays, has been proposed in [14, 15]; high performances sponge-like piezoelectric polymer films are described by [21]. A review of mechanical and electromechanical properties of piezoelectric nanowires is provided in [20]. With reference to the electromechanical transducers, piezoelectric polymers present advantages when large deformations are expected due to the device operating conditions [5, 7, 8]. Piezo-polymers can be divided into to three main classes: bulk piezo-polymers, piezo-composites, and voided charged [17]. Liu et al., in [19], fabricated polymer nonwoven fiber fabric devices using a near field electrospinning process. The final size of apparatus is 5 mm, while fiber diameter is around hundreds of nm. Sun et al., in [13], developed microbelts of PVDF for harvesting energy from respiration. The prototype has a thickness of 20 μm, a length of 20 mm and a width of 2 mm. Ico et al. characterized the macroscopic performances of electrospun PVDF thin films with respect to nanofiber dimensions and demonstrated that the mat electric output is enhanced using smaller fibers due to a substantial increase in both piezoelectric constant and Young modulus [12]. Further evidences of this cooperativity effect among fibers have been recently demonstrated through nanoscale indentation experimental tests [16] and multiphysics finite element models [1, 2, 3]. In this perspective, the feasibility of vibration-powered wireless sensor nodes for structural health monitoring, by using PVDF polymers with piezoelectric fibrous microstructure [2], has been studied in [4] and [10]. Moreover, the possibility of harvesting energy from simulated respiration using PVDF microbelts has been demonstrated in [13]. The focus of this paper is on developing numerical methods to predict contact interactions (including adhesion in electromechanical interfaces) extending existing contact element formulations [3]. The aim is to predict the piezomechanical behavior of a novel class of piezoelectric devices made of a large number of polymeric fibers. In particular 2d and 3d contact elements are developed and implemented for the numerical simulation of the electromechanical interaction between contacting nanowires in presence of coupled mechanical and electrical fields.

2. Method

To derive the equations for piezoelectric problems, the strains, stresses and mechanical displacements are respectively denoted by S_{ij}, T_{ij} and u_i, while E_i and D_i are the electric field and displacement. Navier equations assumes that $T_{ij,j} = 0$ with the condition $T_{ij} = T_{ji}$ for $i \neq j$. The strain-displacement relations states that: $S_{ij} = \frac{1}{2}\left(u_{i,j} + u_{i,j}\right)$. Finally the constitutive equations are: $T_{ij} = C_{ijkl}S_{kl} - e_{kij}E_k$ and $D_i = e_{ikl}S_{kl} - \epsilon_{ik}E_k$ where C_{ijkl}, e_{ikl}, and ϵ_{ik} are respectively the elastic, piezoelectric, and permittivity constants. The last are obtained starting from a potential energy function: $H = \frac{1}{2}S_{ij}S_{kl}C_{ijkl} - \frac{1}{2}E_iE_k\epsilon_{ik} - S_{kl}E_ie_{ikl}$. If ϕ is the electric potential, Gauss and Faraday laws for the electrostatic field become: $D_{i,i} = 0$ and $E_i = -\phi_{,i}$. The boundary conditions for the mechanical field are: $u_i = \bar{u}_i$ on Γ_u and $t_i = T_{ij}n_j = \bar{t}_i$ on Γ_t where $\Gamma = \Gamma_u \cup \Gamma_t$, $\Gamma_u \cap \Gamma_t = \varnothing$, with Γ as the boundary of the domain. The boundary conditions for the electric field are $\phi = \bar{\phi}$ on Γ_ϕ and $d = D_in_i = \bar{d}$ on Γ_d where $\bar{\phi}$ and $\bar{d}$ are prescribed values of electric potential and electric charge flux, and $\Gamma = \Gamma_\phi \cup \Gamma_d$, $\Gamma_\phi \cap \Gamma_d = \varnothing$. Using standard finite element procedures, the displacement field $\mathbf{u}$ and the electric potential ϕ can be defined in terms of shape function matrices $\mathbf{N}_u$ and $\mathbf{N}_\phi$ and nodal values vectors $\hat{\mathbf{u}}$ and $\hat{\boldsymbol{\phi}}$. The final finite element equations governing the electromechanical problem are obtained in the form: $\mathbf{K}_{uu}\hat{\mathbf{u}} + \mathbf{K}_{u\phi}\hat{\boldsymbol{\phi}} = \hat{\mathbf{t}}$ and $\mathbf{K}_{u\phi}{}^T\hat{\mathbf{u}} - \mathbf{K}_{\phi\phi}\hat{\boldsymbol{\phi}} = \hat{\mathbf{d}}$ where $\mathbf{K}_{uu}$, $\mathbf{K}_{u\phi}$, $\mathbf{K}_{\phi\phi}$ are the mechanical, piezoelectric and electrical stiffness matrices. $\hat{\mathbf{t}}$ and $\hat{\mathbf{d}}$ are vectors due to mechanical and electrical load contributions. According to this formulation, both solid 8-nodes brick element and solid 4-nodes plane stress and plane strain elements are implemented in the finite element program AceFEM using the automated derivation of the finite element equations available in AceGen.

Both node-to-segment (NTs) and node to surface (NTS) strategies are used to describe the contact interactions at the interface between two piezoelectric bodies. The aim is to solve 2D and 3D electromechanical frictionless contact problems with adhesion. The contact formulations are based on the master-slave concept while the contact element comprises 3 nodes, i.e. one slave node + two nodes belonging to the master surface for the 2D case and 5 nodes, i.e. one slave node + four nodes belonging to the master surface for the 3D case. The global unknowns are thus the displacements and the electrical potential of these nodes. The impenetrability condition and the electrical condition of equal potential are both regularized with the penalty method and thus enforced by introducing penalty contributions to the potential. Furthermore, a simple adhesion constitutive law is also added to take into account a sticking behaviour between piezoelectric nanowires during a transition between a compressive load to the traction. For each slave node, the normal gap is computed as: $g_N = (\mathbf{x}^s - \bar{\mathbf{x}}^m) \cdot \bar{\mathbf{n}}$ where $\mathbf{x}^s$ is the position vector of the slave node, $\bar{\mathbf{x}}^m$ is the position

vector of its normal (i.e. minimum distance) projection point onto the master surface, and $\bar{\mathbf{n}}$ is the outer normal to the master surface at the projection point. The sign of the measured gap is used to discriminate between active and inactive contact conditions, a negative value of the gap leading to active contact. The electric field requires the definition of the contact electric potential jump: $g_\phi = \phi^s - \bar{\phi}^m$ where ϕ^s and $\bar{\phi}^m$ are the electric potential values in the slave node and in its projection point on the master surface. If ρ_{mech} and ρ_{el} are the penalty parameters and g_N and g_ϕ are the mechanical and electrical gaps, the contact force term is: $F_N = \rho_{\text{mech}} g_N$ and the electric current term is: $I_N = \rho_{\text{el}} g_\phi$. The energy potential contributions due to mechanical contact is $\Pi_M^c = \frac{1}{2} F_N g_N$ and due to electric contact: $\Pi_E^c = \frac{1}{2} I_N g_\phi$. Therefore, the total potential energy contribution due to contact is: $\Pi_{\text{Contact}} = \Pi_M^c + \Pi_E^c$. According to standard variational techniques, the global set of equations can be obtained by adding to the variation of the energy potential representing the continuum behavior the virtual work due to the electromechanical contact contribution provided by the active contact elements. The full set of equations is nonlinear due to the unilateral contact conditions. Consistent linearization of the contribution of the active contact elements is necessary to achieve an asymptotically quadratic convergence rate. Advanced symbolic computational tools available in the AceGen-AceFem finite element environment allow to automate the linearization process above introduced. In particular, if the global energy of the discretized system Π_{global} is defined as: $\Pi_{\text{global}} = \cup H(u, \phi) + \underset{\text{active}}{\cup} \Pi_{\text{Contact}}$ and if $\hat{\boldsymbol{u}}$ is a set of degrees of freedom (DOFs) used to discretize the displacement field $\boldsymbol{u}$ and $\hat{\boldsymbol{\phi}}$ is a set of DOFs used to discretize the electric potential field ϕ and $\hat{\boldsymbol{u}} \cup \hat{\boldsymbol{\phi}}$ is the vector of all nodal DOFs, the residual vector and the stiffness matrix terms resulting from the finite element discretization are determined according to these formulas: $R_{u_i} = \frac{\delta \Pi_{\text{global}}}{\delta \hat{u}_i}$, $R_{\phi_i} = \frac{\delta \Pi_{\text{global}}}{\delta \hat{\phi}_i}$, $K_{\text{uu}_{i,j}} = \frac{\delta R_{u_i}}{\delta \hat{u}_i}$, $K_{\phi\phi_{i,j}} = \frac{\delta R_{\phi_i}}{\delta \hat{\phi}_j}$, $K_{\text{u}\phi_{i,j}} = \frac{\delta R_{u_i}}{\delta \hat{\phi}_j}$, $K_{\phi\text{u}_{i,j}} = \frac{\delta R_{\phi_i}}{\delta \hat{u}_j}$.

3. Results

In this section, three different case studies are discussed. The systems are modelled with the finite element method in order to predict the voltage, displacement, strain and stress distributions in the solids under application of an external pressure or traction. The non-linear problems are consistently linearized with the automatic differentiation technique and solved using an incremental displacement-control procedure with adaptive time-stepping. First of all, it is analyzed a simple 2D indentation problem with adhesion where a small elastic box is pull out from a large elastic box. The material parameters used in the analysis are given in [1] and a load control procedure is used. Figure 1 shows the mesh employed in the analysis for the upper (body 1, slave) and bottom (body 2, master) elements. The contour plots of the total displacement and the electrical voltage are also provided. Second, to benchmark the use of
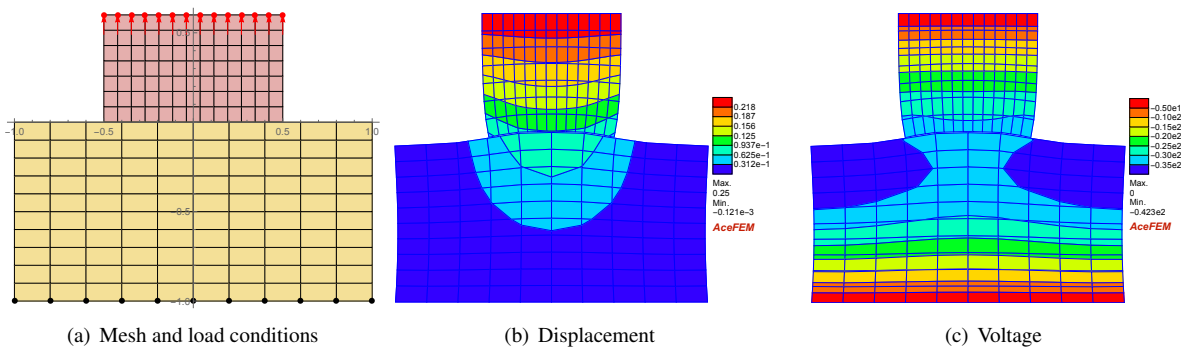

(a) Mesh and load conditions   (b) Displacement   (c) Voltage

Fig. 1. Countour levels of displacement and voltage distributions in the contact between two piezoelectric bodies due to traction (with adhesion) loads at the interface.

quadrilateral 3D contact elements with adhesion, we analyze a 3D indentation problem where again a small elastic box in adhesion with a substrate is subjected to a traction distributed load on his top. Again, the contour plots of the total displacement and the electrical voltage are given in Figure 2. Third, a group of piezoelectric polymer fibers is considered. In the numerical model, the cylinders (representing the fibers) are considered as linear piezoelastic solids,

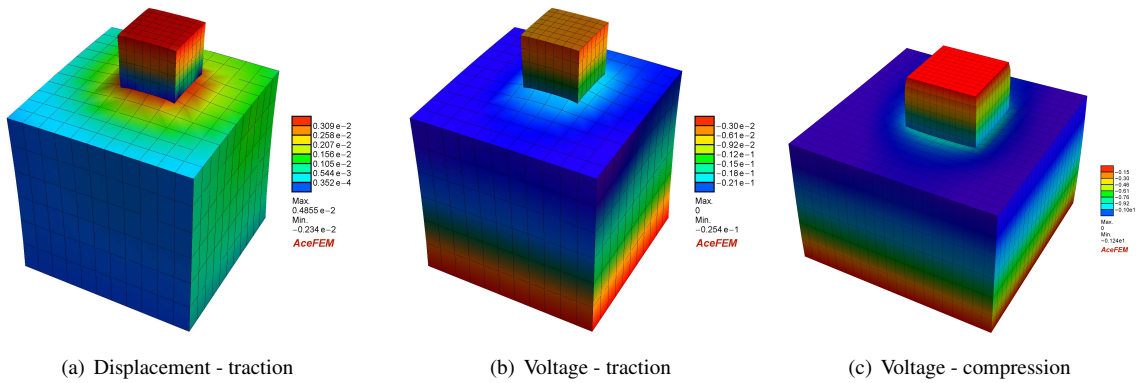(a) Displacement - traction (b) Voltage - traction (c) Voltage - compression

Fig. 2. Countour levels of displacement and voltage distributions in the contact between two piezoelectric bodies due to respectively compression and traction (with adhesion) loads at the interface.

while the loading platens are assumed rigid. The compression is applied under displacement control giving a total displacement to the platens up to 10% of the cylinder radius. Frictionless electromechanical contact constraints are enforced at the interface between each nanowire and also between the platens and the fibers. The fibers are discretized with linear 8-node brick elements. For the treatment of the contact problem in the discretized setting, the NTS contact formulation described above is employed. The penalty parameters for the mechanical and for the electric contributions are taken avoiding ill-conditioning of the global stiffness matrix. In Figures 3 and 4, results are obtained for several arrangement of fibers (namely 1 to 5 fibers in contact) in terms of contour plots of the predicted electrical voltage.
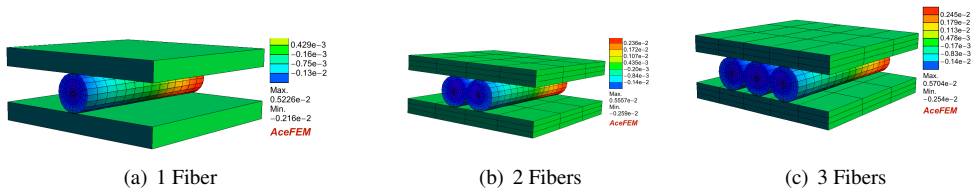

(a) 1 Fiber (b) 2 Fibers (c) 3 Fibers

Fig. 3. Countour levels of voltage distribution in the fibers.
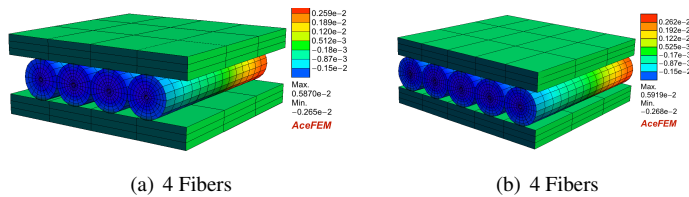

(a) 4 Fibers (b) 4 Fibers

Fig. 4. Countour levels of voltage distribution in the fibers.

4. Conclusion

Numerical modeling of electromechanical interactions at the interface of two piezoelectric deformable bodies during contact is an important aspect to understand and optimize the response of mems and nems systems for sensing and
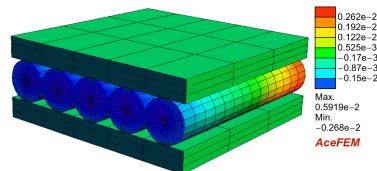
Fig. 5. Microscale behavior, countour levels of voltage distribution in the fibers.

energy harvesting on multiple scales. To fulfill this task, computationally efficient numerical algorithms are important as well as a physically correct definition of the interfacial phenomena. Two contact element formulations based on the note to segment and the node to surface strategies are here derived and implemented in a robust and cost efficient way within an implicit FE method scheme. The electromechanical interactions between nanowires in electrospun fibers based devices are finally predicted since are very important to fully characterize and understand the effect of fiber arrangement on the macroscopic response. The symbolical approach is widely used to generate the contact elements using automatic differentiation for the linearization and code optimization. C^0 continuity during the contact simulations based on implicit methods results sometimes in loss of convergence, therefore future work will focus on including the adhesion features also in contact elements using smooth C^1 interpolations of the contact surfaces.

References

[1] Maruccio C. and De Lorenzis L. (2014) *Numerical homogenization of piezoelectric textiles for energy harvesting*. Fract. Struct. Integr., 1, 49–60.

[2] Persano L., Dagdeviren C., Maruccio C., De Lorenzis L. and Pisignano D. (2014). *Cooperativity in the enhanced piezoelectric response of polymer nanowires*. Adv. Mater., 26, 7574–80.

[3] Maruccio C., De Lorenzis L., Persano L. and Pisignano D. (2015). *Computational homogenization of fibrous piezoelectric materials*. Computational Mechanics, 55, 983–98.

[4] Maruccio C., Quaranta G., De Lorenzis L. and Monti G. (2016). *Energy harvesting from electrospun piezoelectric nanofibers for structural health monitoring of a cable stayed bridge*. Smart Materials and Structures 25(8): 085040.

[5] Maruccio C., Quaranta G., Montegiglio P., Trentadue F. and Acciani G. (2018). *A Two Step Hybrid Approach for Modeling the Nonlinear Dynamic Response of Piezoelectric Energy Harvesters*. Hindawi, Shock and Vibration, pp. 1–22.

[6] Quaranta G., Trentadue F., Maruccio C., Marano G.C. (2018). *Analysis of piezoelectric energy harvester under modulated and filtered white Gaussian noise*. Mechanical Systems and Signal Processing, Volume 104, Pages 134-144.

[7] Maruccio C., Montegiglio P., Acciani G., Carnimeo L., Torelli F. (2018). *Identification of Piezoelectric Energy Harvester Parameters Using Adaptive Models*. 2018 IEEE International Conference on Environment and Electrical Engineering, Palermo, 1–5.

[8] Maruccio, C., Quaranta, G. and Grassi, G. (2019). *Reduced-order modeling with multiple scales of electromechanical systems for energy harvesting*. Eur. Phys. J. Spec. Top. 228, 1605–1624. https://doi.org/10.1140/epjst/e2019-800173-x

[9] Kefal A., Maruccio C., Quaranta G., Oterkus E. (2019). *Modelling and parameter identification of electromechanical systems for energy harvesting and sensing*. Mechanical Systems and Signal Processing, Volume 121, 15 April 2019, Pages 890-912.

[10] Trentadue F., Quaranta G., Maruccio C. and Marano G. C. (2019). *Energy harvesting from piezoelectric strips attached to systems under random vibrations*. Smart Structures and Systems, Volume 24, Number 3, September 2019, Pages 333-343

[11] Montegiglio P., Maruccio C., Acciani G., Rizzello G., Seelecke S. (2020). *Nonlinear multi-scale dynamics modeling of piezoceramic energy harvesters with ferroelectric and ferrolelastic hysteresis*. Nonlinear Dynamics, 2020, accepted.

[12] Ico G., Showalter A., Bosze W., Gott S.C., Kim B.S., Rao M.P., Myung N.V., Nam J. (2016). *A Systematic Approach to Optimize Size-Dependent Piezoelectric and Mechanical Properties of Electrospun P(VDF-TrFE) Nanofibers for Enhanced Energy Harvesting*. Journal of Materials Chemistry A.

[13] Sun C., Shi J., Bayerl D.J., Wang X. (2011). *PVDF microbelts for harvesting energy from respiration*. Energy and Environmental Science, 4(11), 4508.

[14] Koka A., Sodano H.A. (2014). *A Low-Frequency Energy Harvester from Ultralong, Vertically Aligned BaTiO Nanowire Arrays*. Advanced Energy Materials, 4(11).

[15] Koka A., Sodano H.A. (2013). *High-sensitivity accelerometer composed of ultra-long vertically aligned barium titanate nanowire arrays*. Nature Communications, 4.

[16] Gao M., Li L., Li W., Zhou H., Song Y. (2016). *Direct Writing of Patterned, Lead-Free Nanowire Aligned Flexible Piezoelectric Device*. Advanced Science, 3(8).

[17] Ramadan K., Sameoto D., Evoy S. (2014). *A review of piezoelectric polymers as functional materials for electromechanical transducers*. Smart Materials and Structures, 23(3).

[18] Fan F.R., Tang W., Wang Z.L. (2016). *Flexible Nanogenerators for Energy Harvesting and Self-Powered Electronics.* Advanced Materials, 28(22), 4283–4305.

[19] Liu Z.H., Pan C.T., Lin L.W., Huang J.C., Ou Z.Y. (2014). *Direct-write PVDF nonwoven fiber fabric energy harvesters via the hollow cylindrical near-field electrospinning process.* Smart Materials and Structures, 23(2).

[20] Horacio D. Espinosa, Rodrigo A. Bernal, Majid Minary-Jolandan. (2012). *A Review of Mechanical and Electromechanical Properties of Piezoelectric Nanowires.* Advanced Materials, 24(34).

[21] Mao Y., Zhao P., McConohy G., Yang H., Tong Y., Wang X. (2014). *Sponge-Like Piezoelectric Polymer Films for Scalable and Integratable Nanogenerators and Self-Powered Electronic Systems.* Advanced Energy Materials, 4(7).

[22] Park K., Lee M., Liu Y., Moon S., Hwang G.T., Zhu G., Kim J.E., Kim S.O., Kim D.K., Wang Z.L., Lee K.J. (2012). *Flexible Nanocomposite Generator Made of BaTiO3 Nanoparticles and Graphitic Carbons.* Advanced Materials, 24(22).